CHAPTER 172

A NEW TYPE OF BREAKWATER UTILIZING AIR COMPRESSIBILITY

Masaaki IKENO*
Naokatsu SHIMODA**
and
Koichiro IWATA***

ABSTRACT

This paper is to investigate both theoretically and experimentally the wave energy dissipation and air-pressure variation of a new type of breakwater having a pressurized air-chamber and two buoyancy tanks. The theoretical models are developed in this paper and they are shown to be in good agreement with experimental values. The new type of breakwater proposed in this paper is pointed out to attenuate the transmitted wave much better than the rectangular-shaped and concave-shaped breakwaters without the air-chamber.

1. INTRODUCTION

Development of a new type of breakwater having a high sea water exchange and wave energy dissipation is strongly required from environmental and disaster prevention viewpoints.

This paper deals with a new type of fixed breakwater which has one pressurized air-chamber and two buoyancy tanks. The great merit of the breakwater lies in the function that the resonant period can be easily adjusted only by changing the air pressure in the air-chamber without changing the geometrical shape of breakwater itself.

So far, Kiyokawa and Ohyama (1986) and Iwata et al. (1987) have discussed the wave attenuation of the breakwater with a pressurized air-chamber. There still remain, however, problems to be solved from theories and experiments.

* M.Eng., Research Engineer, Central Research Institute of Electrical Power Industry, Abiko, Chiba, Japan
** B.Eng., Vice-Head, General Technical Research Laboratory, Gikenkogyo Co. Ltd.,Hachiohji, Tokyo, Japan
*** D.Eng., Professor, Dept. of Civil Eng., Nagoya Univ., Nagoya, Aichi 464, Japan.

First of all, two theoretical models based on the Dividing Region and Source Distribution Function Methods are newly developed, which take account of air compressibility in the air-chamber. Secondary, laboratory experiments are performed not only to examine the validity of the proposed theoretical models, but also to reveal the characteristics of wave energy dissipation and variation of air pressure in the air-chamber.

2. THEORETICAL MODELS

The Dividing Region Method and Source Distribution Function Method are employed to evaluate changes of wave and air pressure in the air-chamber. The wave treated here is a two-dimensional and irrotational small amplitude one. The fluid is assumed to be inviscid.

2-1. Dividing Region Method

The fluid domain is divided into five regions, as shown in Fig.1. The region I includes the incident and reflected waves and evanescent mode waves, and the transmitted wave exists in the region, V. The air pressure head R in the region III changes with wave motion. Extending the analytical treatment proposed by Iwata et al. (1986), velocity potentials in the five regions are expressed by the following:

$$\phi_1 = (A_o e^{ik(x-\ell_2)} + B_o e^{-ik(x-\ell_2)}) \frac{\cosh k(h+z)}{\cosh kh} + \sum_{n=1}^{\infty} B_n e^{-k_n(x-\ell_2)} \frac{\cos k_n(h+z)}{\cos k_n h} \quad \text{---} \; (1)$$

$$\phi_2 = C_o x + D_o + \sum_{s=1}^{\infty} \left(C_s \sinh\frac{s\pi x}{(1-q_1)} + H_s \cosh\frac{s\pi x}{(1-q_1)}\right) \cos\left(\frac{s\pi(h+z)}{(1-q_2)h}\right) \quad \text{------} \; (2)$$

$$\phi_3 = (E_o e^{ik'x} + F_o e^{-ik'x})\left(\frac{\cosh k'(h+z)}{\cosh k'h}\right) + \sum_{m=1}^{\infty} (E_m e^{k'_m x} + F_m e^{-k'_m x})\left(\frac{\cos k'_m(h+z)}{\cos k'_m h}\right) + \frac{iP_o}{\rho\sigma} \quad \text{------} \; (3)$$

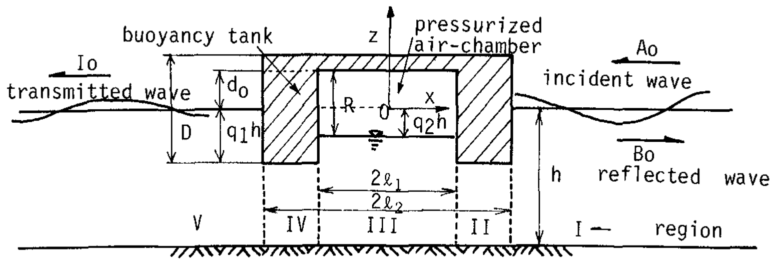

Fig.1 Shematic illustration of new type of breakawter with pressurized air-chamber and two buoyancy tanks and illustration of symboles

$$\phi_4 = G_o x + H_o + \sum_{s=1}^{\infty}\left(G_s \sinh\frac{s\pi x}{(1-q_1)h} + H_s\frac{s\pi x}{(1-q_1)h}\right)\cos\left(\frac{s\pi(h+z)}{(1-q_1)h}\right) \quad \text{--------- (4)}$$

$$\phi_5 = I_o e^{ik(x+\ell_2)}\left(\frac{\cosh k(h+z)}{\cosh kh}\right) + \sum_{n=1}^{\infty}\left(I_n e^{k_n(x+\ell_2)}\left(\frac{\cos k_n(h+z)}{\cos k_n h}\right)\right) \quad \text{--------- (5)}$$

Here, $\phi_1,\phi_2,\phi_3,\phi_4$ and ϕ_5 are,respectively,the velocity potentials in the regions, I, II, III,IV and V,Ao the complex amplitude of incident wave $(=igH_I/2\sigma)$; g the gravitational acceleration, H_I the incident wave height; i imaginary unit number; σ the angular frequency $(=2\pi/T)$; T the wave period, B_o the complex amplitude of reflected wave; I_o the complex amplitude of transmitted wave; $B_n,C_s,D_s,E_m,F_m,G_s,H_s$ and I_n (n=1, 2,3,--, s=m=0,1,2,--) complex unknown coefficients; h the still water depth; x the horizontal axis; z the vertical axis; k,k_n,k' and k'_m the wave numbers satisfying the relationship of $\sigma^2/g= k \tanh kh = -k_n \tan k_n h = k' \tanh k'(1-q_2)h = -k'_m \times \tan k'_m(1-q_2)h$; ρ the density of water; Po the air pressure amplitude in the air-chamber ; $2\ell_2$ the length of air-chamber; $2\ell_2$ the length of breakwater; $q_1 h$ the submerged depth of breakwater.

(b) Air pressure amplitude Po

The 5th term, $iPo/\rho\sigma$ in Eq.(3) is the pressure term added by compressibility of air in the air-chamber. In deducing Eq.(3), the air pressure,P_a in the air-chamber is expressed as

$$P_a = \overline{P}o + Poe^{i\sigma t}, \quad (\overline{P}o=\rho g q_2 h + P_{air}) \quad \text{------ (6)}$$

where, $\overline{P}o$ is the initial air pressure and P_{air} the atomospheric pressure. The linearized dynamic boundary condition on the free surface in the air-chamber is

$$\eta = -i\frac{\sigma}{g}\phi_3 - \frac{P_a}{\rho g} \quad \text{------------- (7)}$$

where,η is the free surface elevation from the still water level.

Substitution of Eqs.(3) and (6) into Eq.(7) and assumption of uniform rise and fall of water surface in the air-chamber yield

$$\eta = -q_2 h + \eta_o e^{i\sigma t},$$

$$\eta_o = \frac{1}{2l_1}\int_{-\ell_1}^{\ell_1}\left(-i\frac{\sigma}{g}(Ee^{ik'x}+Fe^{-ik'x})\left(\frac{\cosh k'(1-q_2)h}{\cosh k'h}\right)dx\right. \quad \text{----------- (8)}$$

The volume of air, V in the air-chamber is given by

$$V = Vo - \eta_o e^{i\sigma t}, \qquad Vo = d_o + q_2 h \quad \text{-------- (9)}$$

where, Vo is the initial volume of air in the air-chamber and d_o the clearance of the upper plate from the still water level at the region, I and V (see Fig.1).

Assuming the adiabatical change of air in the air-chamber, the air pressure P_a corresponding to air volume of V is given by

$$P_a = \overline{P}o(Vo/V)^r, \quad (r = 1.4) \quad \text{-------- (10)}$$

Linearization after substitution of Eqs.(6) and (9) into Eq.(10) yields

$$Po = r\overline{P}o(\eta_o/do + q_2h)) \qquad \text{------------- (11)}$$

(c) Matching condition

The continuity of pressure, P and horizontal particle velocity, u is employed as the matching condition at the boundary between two regions (i.e., $x = \ell_1, \ell_2, -\ell_1$ and $-\ell_2$). The pressure, P_j,(j=1 - 5) and horizontal velocity of water particle, u_j, (j=1 - 5) are estimated with

$$\left.\begin{aligned} P_j(x,z;t) &= -\rho gz - i\rho\sigma\phi_j(x,z)e^{i\sigma t} \\ u_j(x,z;t) &= \frac{\partial}{\partial x}(\phi_j)e^{i\sigma t} \end{aligned}\right\} \qquad \text{------- (12)}$$

where, subsuffix j indicates the region, j.

$$\left.\begin{aligned}
&\text{(i) } x = \ell_2 && P_1(\ell_2,z;t) = P_2(\ell_2,z;t) && ;\ (-h\leq z\leq -q_1h) \\
& && u_1(\ell_2,z;t) = 0 && ;\ (-q_1h<z\leq 0\ ) \\
& && \qquad = u_2(\ell_2,z;t) && ;\ (-h\leq z\leq -q_1h) \\
&\text{(ii) } x = -\ell_2 && P_5(-\ell_2,z;t)=P_4(-\ell_2,z;t) && ;\ (-h\leq z\leq -q_1h) \\
& && u_5(-\ell_2,z;t)=0 && ;\ (-q_1h<z\leq 0) \\
& && \qquad =u_4(-\ell_2,z;t) && ;\ (-h\leq z\leq -q_1h) \\
&\text{(iii) } x= \ell_1 && P_3(\ell_1,z;t) =P_2(\ell_1,z;t) && ;\ (-h\leq z\leq -q_1h) \\
& && u_3(\ell_1,z;t) =0 && ;\ (-q_1h<z\leq -q_2h) \\
& && \qquad =u_4(\ell_1,z;t) && ;\ (-h\leq z\leq -q_1h) \\
&\text{(iv) } x = -\ell_1 && P_3(-\ell_1,z;t)=P_2(-\ell_1,z;t) && ;\ (-h\leq z\leq -q_1h) \\
& && u_3(-\ell_1,z;t)=0 && ;\ (-q_1h<z\leq -q_2h) \\
& && \qquad =u_4(-\ell_1,z;t) && ;\ (-h\leq z\leq -q_1h)
\end{aligned}\right\}$$

$$\text{-------(13)}$$

Since Ao is given as $igH_I/2\sigma$ (known value), the unknowns of $B_n, C_s, D_s, E_m, F_m, G_s, H_s$ and I_s (n=s=m=0,1,2,3,---) are determined by solving Eq.(13) with help of Eqs.(1) through (12). The reflection coefficient, r_R and transmission coefficient, r_T are defined by $|Bo/Ao|$ and $|Io/Ao|$, respectively.

2-2. Sourse Distribution Function Method

The velocity potential in the fluid, $\phi(x,z)$ is expressed by the sum of the incident wave velocity potential, ϕ_I and the scattered wave one, ϕ_D and ϕ_D is given by a function of the Green function, G and the source distirbution function, f as follows (Nakamura et al.(1982));

$$\left.\begin{aligned}
\phi(x,z) &= \phi_I(x,z) + \phi_D(x,z) \\
\phi_D &= \int_S f(X,Z)\cdot G(x,z:X,Z)ds(X,Z) \\
G &= \frac{(ik^2-ko^2)e^{ik|x-X|}}{k(hk^2-hko^2+ko)}\cosh k(h+Z)\cosh k(h+z) \\
&\quad -i\sum_{n=1}\frac{(k_n^2+ko^2)e^{-k_n|x-X|}}{k_n(hk_n^2+hko^2-ko^2)}\cos k_n(h+Z)\cos k_n(h+z)
\end{aligned}\right\}$$

$$\text{------ (14)}$$

where, ko is the wave number in deep water; k and k_n the wave number satisfying the relationship of $\sigma^2/g = k_0 = k \tanh kh = -k_n \tan k_n h$; x the horizontal axis; z the vertical axis with origin at still water level; X and Z the source point; i the imaginary unit number; h the still water depth; s the boundary having the source points.

Once f is determined, Po, r_R and r_T are easily obtained. The detalied calculation technique is referred to reference 4). In this study, the source points were distributed at the interval of $\Delta s/L=0.02$ along the submerged breakwater surface under water and along the water surface in air-chamber, where Δs is the element length between adjacent two source points and L the wavelength at the depth of h.

3. LABORATORY EXPERIMENTS

3-1. Equipment and procedure

In the experiments, two wave tanks were used. Main parts of experiments were performed in an indoor wave tank in 0.9m height, 0.7m width and 25m length at Nagoya University. A flap-type wave generator controlled by Oil-pressure servo was installed at one end of the tank. The water is perfectly shut out from the area behind the wave board. Therefore, the input electrical signal is smoothly converted to the wave motion. At the other end of wave tank, a wave absorbing slope constructed with crush stone and stainless steel chips was placed so as to reduce the wave reflection to a minimum. A large wave tank in 1.6m height,1m width and 50m length of General Technical Research Laboratory at Gikenkogyo Co.Ldt. was also used to examine the scale effect of model breakwater to the air pressure variation in the air-chamber.

Two model breakwaters made of acrylic plate, as shown in Fig.2, were employed to investigate the wave energy dissipation and air pressure variation in the air-chamber. The other types of breakwater such as concave-shaped and rectangular-shaped ones were also employed in order to discuss the difference in wave attenuation among the three types of breakwater. The submerged depth,q_1h and pressurized head,q_2h adopted in this study are listed in Table 1, which also includs q_1 in case of the concave-shaped and rectangular-shaped breakwaters.

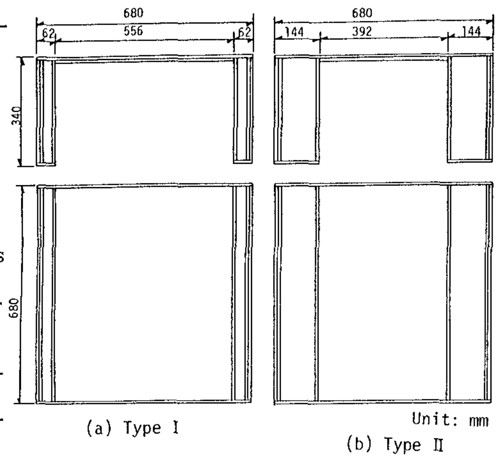

Fig.2 Geometrical scale of model breakwaters with pressurized air-chamber

Water surface profiles were measured with three capacitance-type wave gauges and they were all recorded on a magnetic tape. The transmitted wave was measured with the wave gauge, No.3 which was located at about one wave length distance from back side of

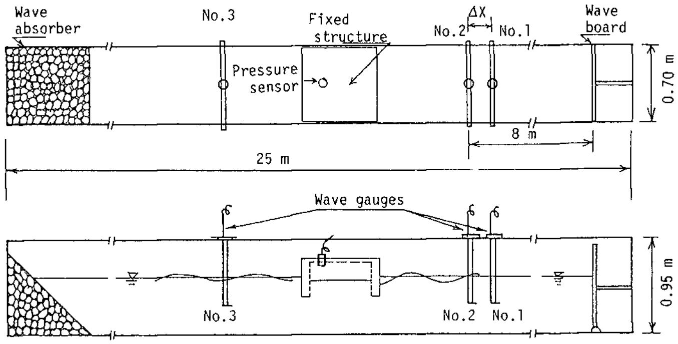

Fig.3 Shemation illustration of experimental set up

Type I pressurized-type (ℓ_1/ℓ_2=0.82, 0.99)

pressurized head q_2h (cm)	draft depth q_1h (cm)
1.1	29.3
2.1	25.3
4.0	17.7
5.2	13.3

Type I' concaved-shaped (ℓ_1/ℓ_2=0.82)

pressurized head q_2h (cm)	draft depth q_1h (cm)
1.1	29.3
2.1	25.3
4.0	17.7
5.2	13.3

Type II (ℓ_1/ℓ_2=0.58)

pressurized head q_2h (cm)	draft depth q_1h (cm)
-1.7	17.7
0.0	15.6
1.8	13.3

Type II' (ℓ_1/ℓ_2=0.58)

pressurized head q_2h (cm)	draft depth q_1h (cm)
-1.7	17.7
0.0	15.6
1.8	13.3

rectangular-shaped

draft depth q_1h (cm)
29.5
25.3
17.7
15.6
13.3

Table 1 Experimental condition for three types of breakwaters (pressurized-type, concave-shaped and rectangular-shaped breakwaters)

the breakwater. The partial standing wave profiles were measured with two wave gauges, No.1 and No.2 in order to calculate the reflection coefficient, r_R. The distance, Δx between the two wave gauges was changed according to the wave period; that is, $\Delta x=(9/8)L$ for T=0.5s, $\Delta x=(7/8)L$ for T=0.6s - 0.8s and $\Delta x=(3/8)L$ for $T \geqq 1.0$s, where L is the wave length at the depth of h. The air pressure in the air-chamber was measured with a pressure gauge (Kyowa PGM-0.5) attached to the top plate in the air-chamber.

All the experimental waves generated in this study were regular ones. The wave period employed was 0.5s,0.6s,0.65s, 0.7s,0.75s,0.8s,0.9s,1.0s,1.2s,1.4s,1.6s,2.0s, and 2.4s. The wave steepness, H/L was 0.01 for q_1=0.488 and 0.02 for q_1=0.222,0.295 and 0.422 in order to avoid wave breaking. The still water depth was 60cm throughout the experiments.

Total number of experimental runs was about 300. The experimental set-up and conditions performed in the large wave tank of GTRL at Gikenkogyo Co.Ldt. are not described here, due to limitation of paper. As mentioned above, experiments in the large wave tank were carried out to check the model scale effect to the air pressure in the air-chamber. Based on Froude similarity law, dimensions of model breakwaters, water depth and wave conditions were determined so as to correspond to experiments in small wave tank at Nagoya university. The geometrical scale in the large wave tank was selected as 1.7 times larger than that in the small wave tank. The number of experimental runs in the large wave tank was about 50.

3-2 Data analysis

The wave reflection coefficient, r_R was calculated with two-wave-gauges method (Goda& Suzuki(1976)), using the measured wave profiles at wave gauges No.1 and No.2. The transmission coefficient, r_T was calculated using measured wave height of wave gauge, No.3. The reflection and transmission coefficients, r_R and r_T are defined by H_R/H_I and H_T/H_I, respectively, where H_R, H_T and H_I are the reflected, transmitted and incident wave heights, respectively.

3-3 Results and discussion

Using Dividing Region Method (hereafter referred to as DRM) and Source Distribution Function Method (hereafter referred to as SDFM), theoretical values of wave transmission and reflection coefficients and air pressure variation in the air-chamber were evaluated to compare with experimental values. One example is shown in Fig.4, in which experimental values are also plotted for comparison. Theoretical calculations based on the two methods are in good agreement with experimental values. Difference between theoretical values estimated with DRM and those with SDFM is recognized very small in the range of $2\ell_2/L \leqq 0.6$, which is general feature in this study. Since DRM requires less computatioal time than

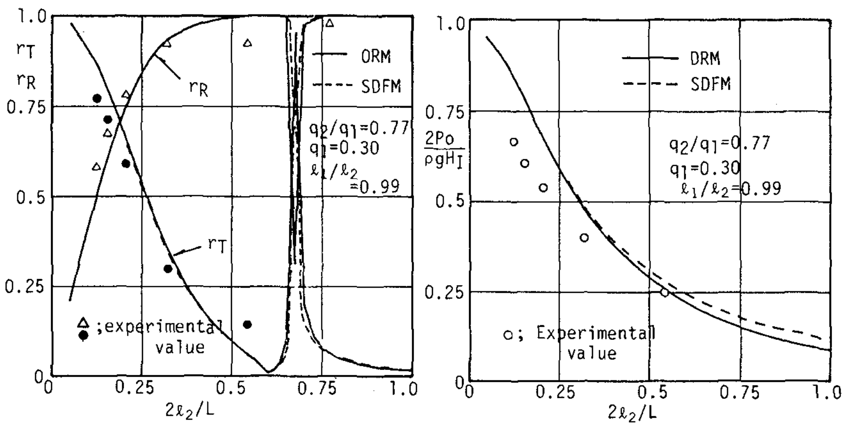

Fig.4 Comparison of theoretically estimated values between Dividing Region Method and Source Distribution Function Method.

SDFM. In addition, theoretical values of $Po/\rho gH_I$ estimated with DRM seem to be in better agreement with experimental values, as shown in Fig.4. Therefore, hereafter, theoretical values evaluated with DRM are employed to compare theory with experiments.

Fig.5 shows changes of the transmission coefficient, r_T and the reflection coefficient, r_R with $2\ell_2/L$. It is seen that the theoretical values agree well with experimental values. The transmission coeffcient, r_T increases with decreasing of $2\ell_2/L$ and q_1. r_T is expected to be less than 0.25 for $2\ell_2/L \geqq 0.3$ in case of $q_1=0.422$, $q_2=0.035$ and $\ell_1/\ell_2=0.82$, as shown in Fig.5(c). On the other hand, the reflection coefficient, r_R decreases with a decrease of q_1 and $2\ell_2/L$. r_R is almost equal to 1 in the range of $2\ell_2/L \geqq 0.8$, which is independent of q_1, q_2, do and ℓ_2/ℓ_1, as shown in Fig.4, in this study.

The effect of initial air pressure, $\overline{P}o$ to r_R and r_T is not clearly recognized. The effect of pressurized head, q_2h to r_R and r_T is not clear too, although r_T seems to become smaller as q_2h becomes larger, as shown in Fig.4. This may be due to the reason that the experimental range of the initial air pressure, $\overline{P}o$ and the pressurized head, q_2h was too narrow to affect r_R and r_T. Concerning the effect of initial air pressure or pressurized head to r_R and r_T, we will discuss later from theoretical calculations with DRM.

Fig.6 shows two examples of variations of the dimensionless air pressure amplitude, $Po/\rho gH_I$ in the air chamber. It can be pointed out, from Fig.6, that theoretical values agree well with experimental values. $Po/\rho gH_I$ increases monotonously as $2\ell_2/L$ becomes smaller. This trend is different from those of r_R and r_T. $Po/\rho gH_I$ measured in the small wave tank is quite equal to those measured in the large wave tank. Then, the model scale effect to $Po/\rho gH$ is not recognized in the two laboratory experiments.

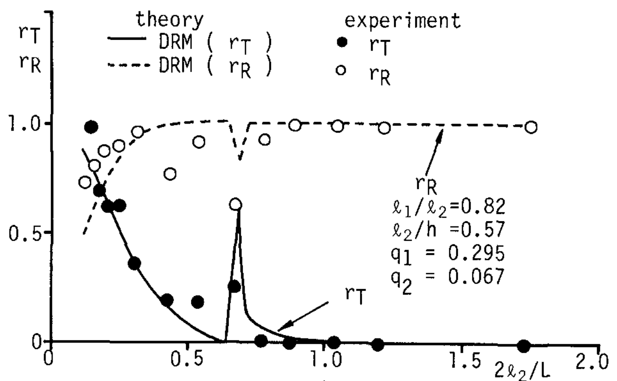

(a)

Fig.5 Comparison between theoretical values and experimental values of r_R and r_T.

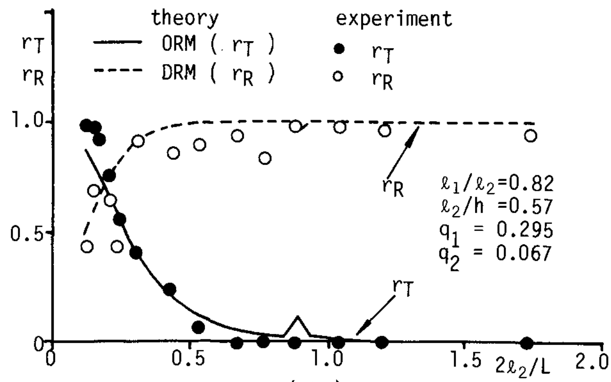

(b)

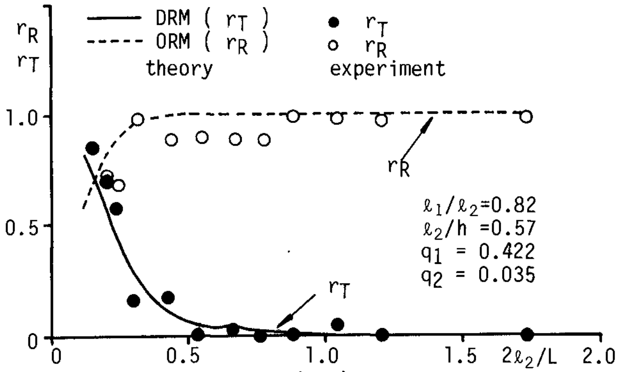

(c)

Fig.5 Comparison between theoretical values and experimental values of r_R and r_T.

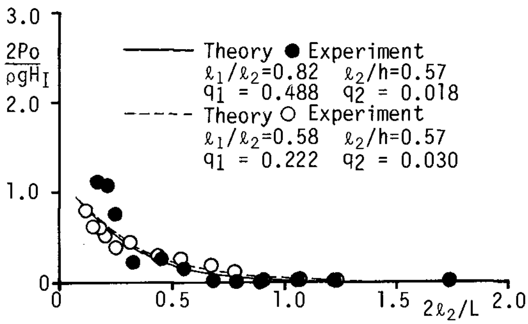

Fig.6 Comparison between theoretical values and experimental values of $Po/\rho gH_I$

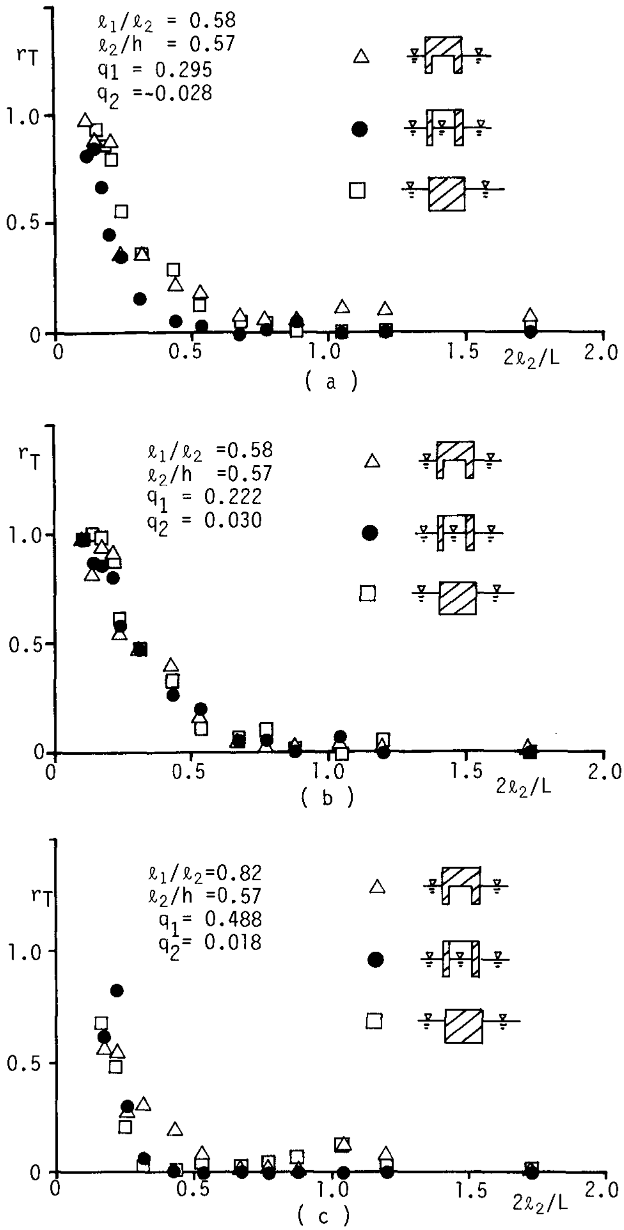

Fig.7 Comparison of transmission coefficient, r_T among pressurized-type, concave-shaped and rectangular-shaped breakwaters

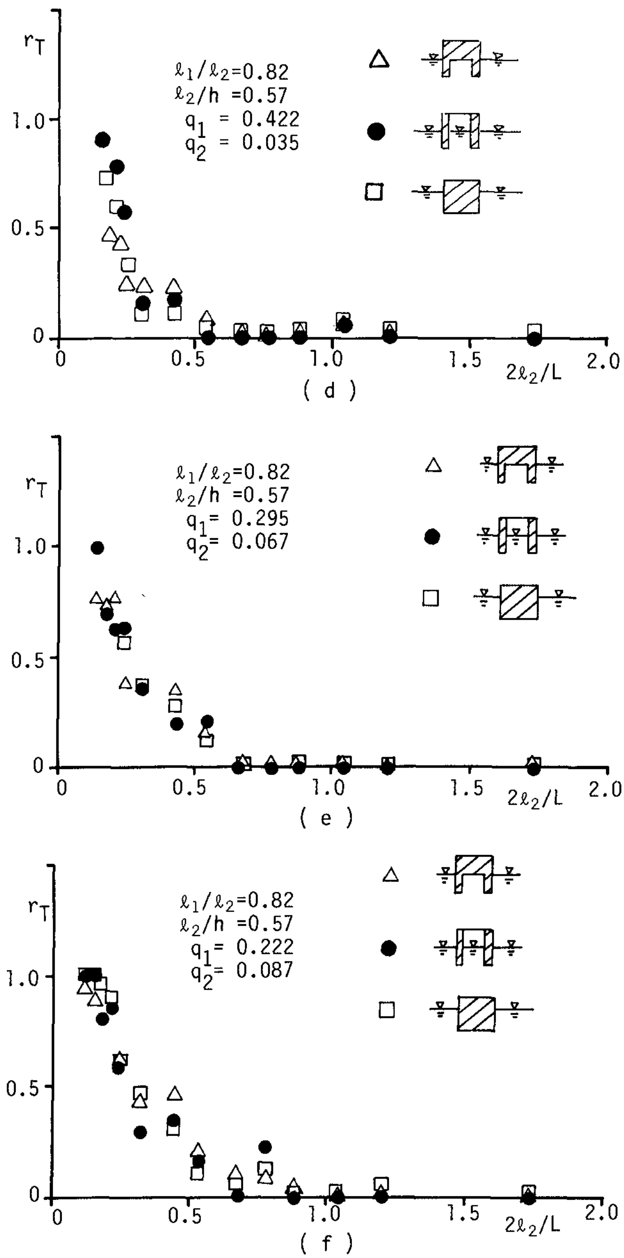

Fig.7 Comparison of transmission coefficient, r_T among pressurized-type, concave-shaped and rectangular-shaped breakwaters

Next, let us discuss the difference in the transmitted wave height due to the new type of breakwater (hereafter referred to as pressurized-type breakwater), and concave-shaped and rectangular-shaped breakwaters.

Figures 7(a)-(f) show experimental results of transmission coefficient, r_T due to the three different types of breakwaters. In each figure, the breakwater length, $2\ell_2$ and draft depth, q_1h are quite the same among the three different types of breakwaters. It is seen that the transmission coefficient, r_T increases largely with decreasing of $2\ell_2/L$ in the range of $2\ell_2/L \leq 0.5$. As shown in Figs.(a)-(f), there are no large difference in r_T due to the pressurized-type, concave-shaped and rectangular-shaped breakwaters. However, r_T of the pressurized-type breakwater are comparatively smaller than those of the concave-shaped and rectangular-shaped breakwaters (see Figs.(a),(b), (e) and (f)). Therefore, it can be pointed out that the pressurized-type breakwater proposed in this study is better than the concave- and rectangular-shaped breakwaters in order to attenuate the transmitted wave.

From engineering viewpoint, r_T is frequently requested to be less than 0.5 for $q_1 \leq 0.5$ and $2\ell_2/L \leq 0.4$. As stated above, since DRM evaluates well the experimental values of r_T due to the pressurized-type breakwater, we will further discuss here, based on theoretical calculations estimated with DRM, the effect of pressurized head, q_2 to r_T and geometrical dimensions of the pressurized breakwater which attenuate r_T less than 0.5 for $q_1 \leq 0.5$ and $2\ell_2/L \leq 0.4$.

Figure 8 indicates that r_T becomes smaller with increasing of the dimensionless pressurized head, q_2/q_1 and r_T becomes minimal at $q_2/q_1=1$. Then, it can be said that increase of the pressurized head is effective to decay the transmission coefficient.

Figures 9(a)-(c) show some cases of optimum geometrical dimensions of the pressurized-type breakwater which can attenuate r_T less than 0.5 for $q_1 \leq 0.5$ and $2\ell_2/L \leq 0.5$. It is said that r_T is also affected by $(1-\ell_1/\ell_2)$ and that r_T decreases as $(1-\ell_1/\ell_2)$ becomes smaller. From Fig.9, combinations of $(1-\ell_1/\ell_2)$, q_1 and $2\ell_2/L$ which attenuate r_T less than 0.5 are found out in case of $q_1/q_2=1.0$ for three relative water depth, $h/L=0.078, 0.131$ and 0.207. Figure 9(c) shows that r_T becomes 0.3 when $q_1=0.5$, $2\ell_2/L=0.28$ and $(1-\ell_1/\ell_2)=0.01$ in case of $q_1/q_2=1.0$ and $h/L=0.207$. Thus, it is possible for this type of breakwater to attenuate r_T less than 0.3 in the case of $q_1=0.5$ and $2\ell_2/L \leq 0.4$.

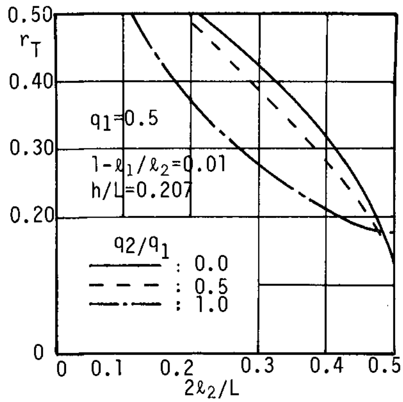

Fig.8 Effect of pressurized head, q_2 to r_T

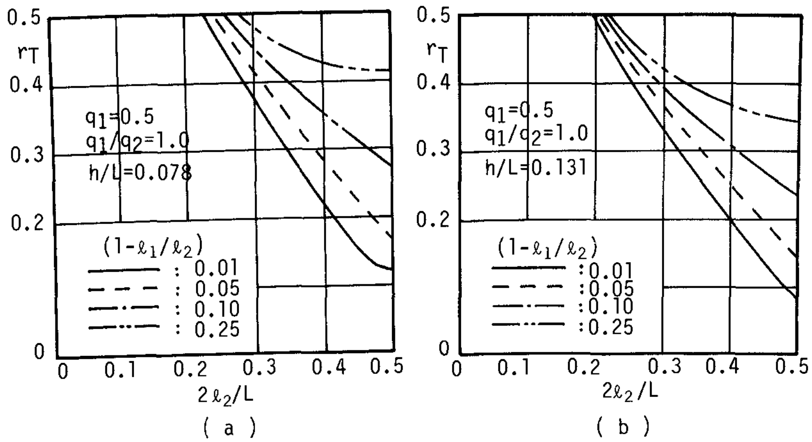

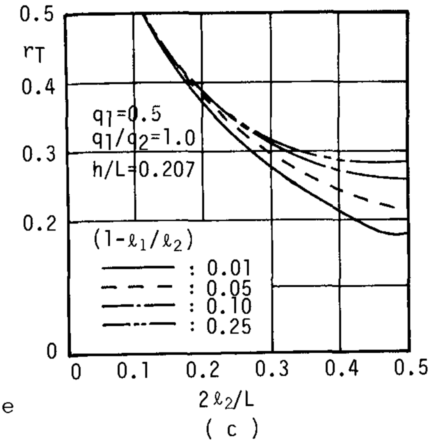

Fig.9 Combinations of $(1-\ell_1/\ell_2)$ and $2\ell_2/L$ which satisfy $r_T \leq 0.5$ within $2\ell_2/L \leq 0.5$ in case of q_1= 0.5 and q_1/q_2=1.0 for h/L=0.078,0.131 and 0.207

4. CONCLUSIONS

Wave reflection and transmission and air pressure in the air-chamber due to a new type of breakwater which has a pressurized air-chamber and two buoyancy tanks have been discussed from theory and laboratory experiments. The main results obtained in this study are summarized as follows:

(1) The theory using the Dividing Region Method is newly developed in order to evaluate the reflection and transmission coefficients and air pressure variation in the pressurized air-chamber. The proposed theory estimates well experimental values.

(2) Theoretical calculations show that the pressurized in the air-chamber plays an important role to attenuate the transmission coefficient,r_T. The transmission coefficient becomes smaller with increasing head in the air-chamber.

(3) The transmission coefficient of the pressurized-type breakwater is comparatively smaller than those of the concave-shaped and rectangular-shaped breakwaters.

(4) The effect of Po to the refelction and transmission coefficients becomes smaller as $2\ell_2/(do+q_1h)$ becomes larger.

(5) Since the wave transmission coefficient due to the

proposed new type of breakwater can be attenuated less than 0.35 for $2\ell_2/L \leqq 0.3$ and $q_1 \leqq 0.5$, there is high possibility that this pressurized-type breakwater will be put into practical use in the sea area where high water exchange and wave decay functions are simultaneously required.

REFERENCES

1) Goda,Y.and Y.Suzuki (1976): Estimation of incident and reflected waves in random wave experiments, Proc.15th ICCE, Hawaii,pp.828-845.
2) Iwata,K.,Oki,M.,Kitaura,S.,Okuoka,T.and M.Ikeno (1986): Motion of floating structure with a pressurized air-chamber, Proc.33rd Japanese Conf.on Coastal Eng.,pp.531-535 (in Japanese).
3) Iwata,K.,Ikeno,M.,Eguro,T.and K.Nakayama (1987): Wave deformation due to structure with a pressurized air-chamber, Abstracts of Ann. Conv., Chubu-Branch of JSCE,pp. 212-213 (in Japanese).
4) Iwata,K.,Ikeno,M.,Nakayama,K.,Ueda,T. and H.Ishii (1988): Numerical programing of motions of structure with a pressurrized air-chamber and two buoyancy tanks in floating, moored and fixed conditions, Technical Rept., Coastal and Ocean Eng. Labo, Dept. of Civil Eng., Nagoya Univ.,pp.II-1 -II-53 (in Japanese)
5) Kiyokawa,S. and T.Ohyama (1986): Wave reflection and transmission due to structure with air-pressurized curtain-wall breakwater, Proc.JSCE,No.375,pp.271-280 (in Japanese).
6) Nakamura,T.,Takahashi,K. and K.Nakayama (1982): Analytical method of wave deformation and forces around two-dimensional body using source distribution method, Proc.29th Japanese Conf. on COastal Eng.,pp.462-466 (in Japanese).